Electronic Supplementary Material (ESI) for Industrial Chemistry & Materials.

Supporting Information

Polyaniline-derived carbon nanofibers with a high graphitization degree loading ordered PtNi intermetallic nanoparticles for oxygen reduction reaction

Yujuan Zhuang, [a,b] *Jiao Yang,* [b] *Lingwei Meng,* [a,b] *Chuanming Ma,* [b] *Lishan Peng,*[*a,b] *De Chen,* [*c] *Qingjun Chen*[*a,b]

[a] School of Rare Earth, University of Science and Technology of China, Hefei, China

[b] Key Laboratory of Rare Earths, Chinese Academy of Sciences; Ganjiang Innovation Academy, Chinese Academy of Sciences, Ganzhou, China

[c] Norwegian University of Science and Technology, Trondheim, Norway. Email: de.chen@ntnu.no

Content:

1. Experimental Section

1.1. Physical Measurements

Powder XRD patterns were collected over the 2θ range 5-90º on a Bruker D8 Focus X-ray diffractometer equipped with a Cu Kα radiation source (λ = 1.5405 Å). The FT-IR spectra were collected on an infrared spectrometer (Nicolet iS5, ThermoFisher Scientific, USA). Raman spectra were collected on a Renishaw in Via Reflex spectrometer system equipped with a 532 nm laser excitation source. N_2 adsorption-desorption isotherms were acquired at 77 K using a Quadrasorb SI MP apparatus. High resolution transmission electron microscopy (HRTEM) images and high-angle annular dark field scanning TEM (HAADF-STEM) images were collected on a JEOL-2100F transmission electron microscope operating at 200 kV. Aberration-corrected HAADF-STEM images and energy-dispersive X-ray spectroscopy (EDX) spectra were acquired on a JEM-ARM300F S/STEM (JEOL) operating at 300 kV. Inductively coupled plasma-optical emission spectroscopy (ICP-OES, PQ9000, Analytik Jena., Ltd, Germany) was used to quantify the amount of Pt and Ni in the samples. X-ray photoelectron spectroscopy (XPS) data were obtained on a VGESCALABMKII X-ray photo-electron spectrometer using a non-monochromatized Al-Kα X-ray source (hν = 1486.7 eV).

1.2. Electrochemical Measurements

A catalyst (5 mg) was added to 2.5 mL of a mixed solvent (including 2-propanol (2 mL) and water (0.48mL)) and Nafion (20 μL). Al_2O_3 powder (50 nm) was applied to polish the rotating disk electrode (RDE). The prepared ink uniformly covered the surface of the electrode as a thin film. An Autolab electrochemical workstation was used for performance evaluation. Ag/AgCl were regarded as reference electrodes in 0.1 M $HClO_4$. A carbon rod was used as a counter electrode. The indicated potentials are all referred to the reversible hydrogen electrode (RHE). The calculated catalyst loading on the GC surface was 0.102 mg cm^{-2}. All cyclic voltammograms (CVs) and linear sweep voltammograms (LSV) were obtained at a scan rate of 50 mV s^{-1} and 5 mV s^{-1}.

The ORR electron transfer numbers (n) and the peroxide yields (% H_2O_2) were

measured using a rotating ring disk electrode (RRDE), with a glassy carbon disk (0.2472 cm^2) and Pt ring (6.25 mm ring inner diameter, 7.92 mm outer diameter, and a 320 μm ring-disk gap). RRDE measurements were conducted by linear sweep voltammetry (LSV) from 1.1 V to 0.2 V vs. RHE at a scan rate of 10 mV s^{-1} at 1600 rpm, while the ring electrode was held at 1.3 V vs. RHE. The electron transfer number and the % H_2O_2 were calculated from the ring current (I_r) and the disk current (I_d) using the following equations:

$$H_2O_2\% = 200 \times \frac{I_r/N}{I_d + I_r/N}$$

$$n = 4 \times \frac{I_d}{I_d + I_r/N}$$

Where I_d is the Faradaic current at the disk, I_r is the Faradaic current at the ring, and N is the H_2O_2 collection coefficient at the ring (N = 0.37).

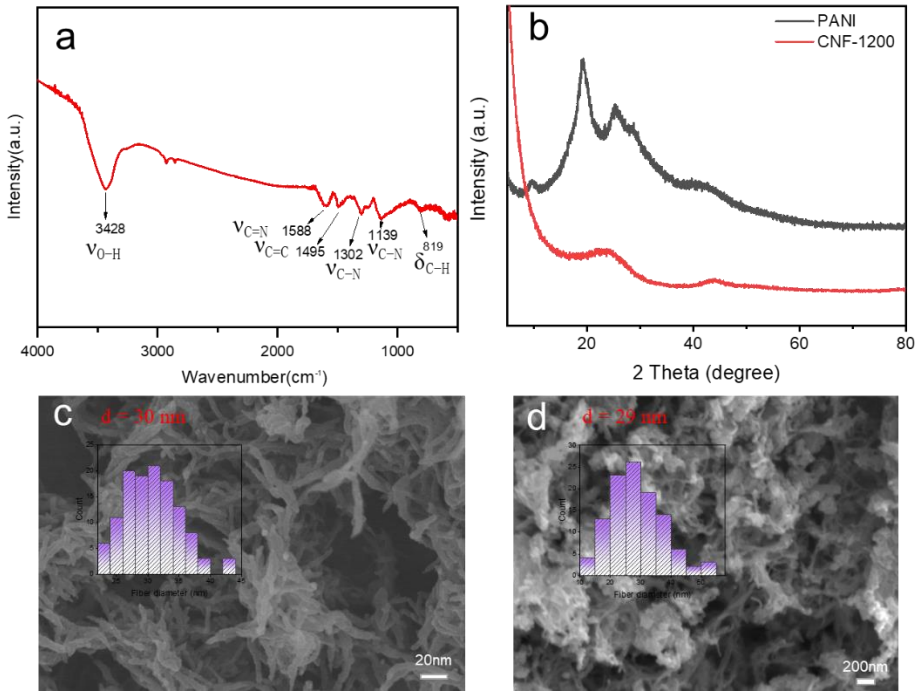

Fig. S1. (a) FTIR spectrum for PANI. (b) XRD patterns for PANI and carbonized PANI. (c) SEM image and distribution of fiber diameter (inset) for PANI. (d) SEM image and distribution of fiber diameter (inset) for CNF-1200.

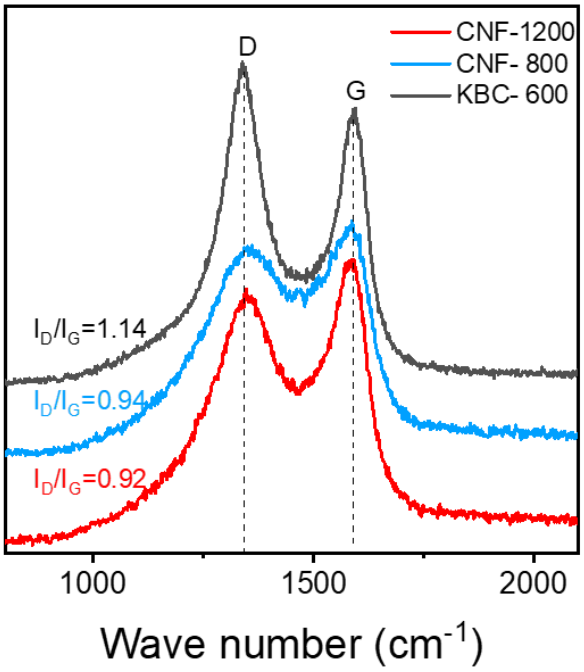

Fig. S2. Raman spectra for CNF-1200, CNF-800 and KBC-600.

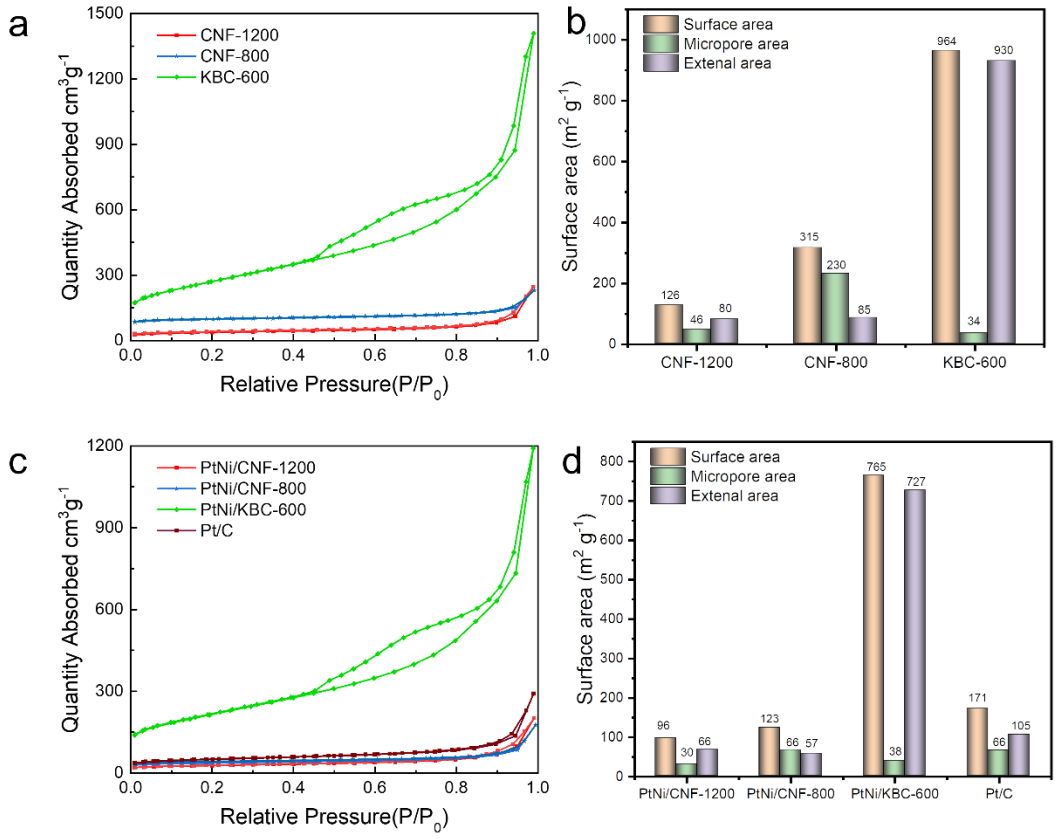

Fig. S3. (a) N_2 adsorption/desorption plots and (b) BET surface areas, micropore surface areas (calculated from pores of diameter <2 nm) and external surface areas (calculated by subtracting the micropore surface areas from the BET surface areas) for CNF-1200, CNF-800 and KBC-600. (c) N_2 adsorption/desorption plots and (d) BET surface areas, micropore surface areas and external surface areas for 20% Pt/C, PtNi/CNF-1200, PtNi/CNF-800, and PtNi/KBC-600.

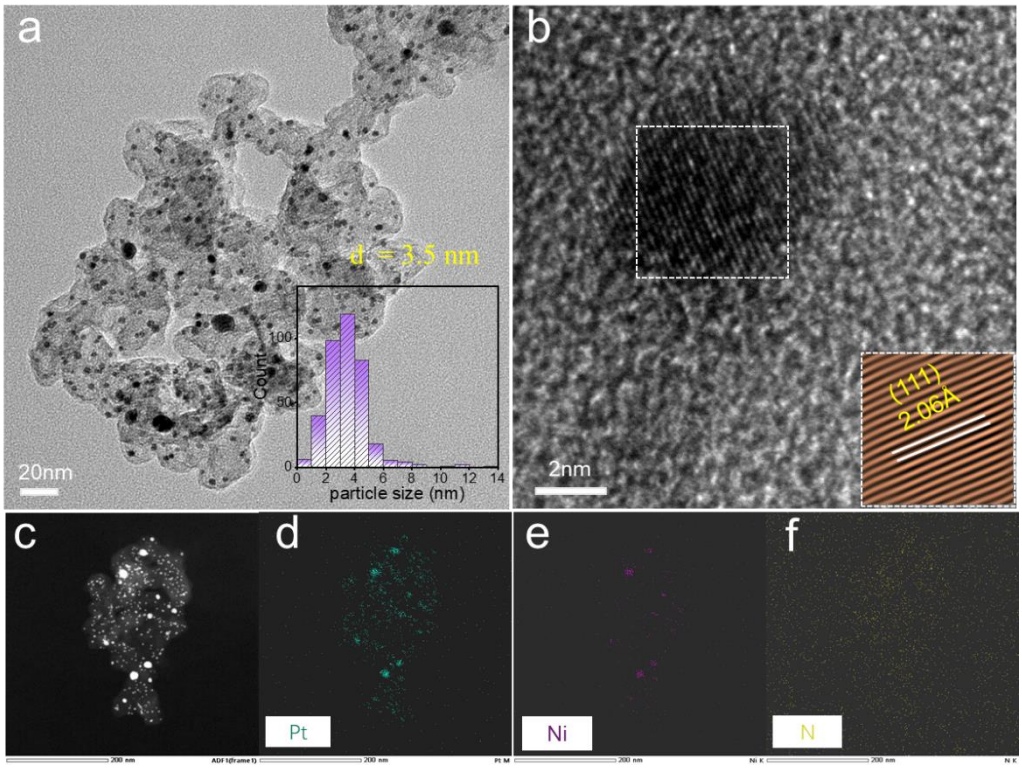

Fig. S4. (a) HRTEM image and particle size distribution (inset), (b) HRTEM image, the inset shows the corresponding information about lattice fringes, (c) HRTEM image and (d-f) energy-dispersive X-ray spectroscopy (EDS) mapping for PtNi/KBC-600.

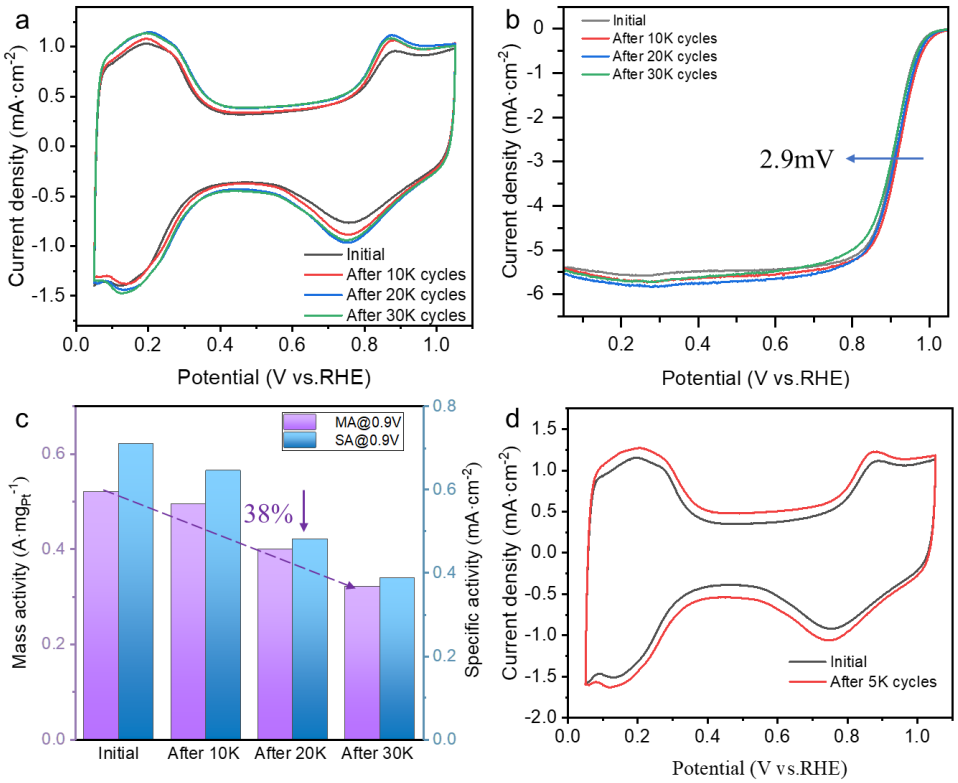

Fig. S5. (a) Cyclic voltammograms before and after different cycle tests in Ar-saturated electrolyte (50 $mV \cdot s^{-1}$), (b) Polarization curves before and after different cycle tests in O_2-saturated electrolyte (5 $mV \cdot s^{-1}$), (c) SA and MA before and after different cycle tests and (d) Cyclic voltammograms before and after 5000 cycles in a high potential range of 1.0–1.5 V for PtNi/CNF-1200 in O_2-saturated electrolyte.

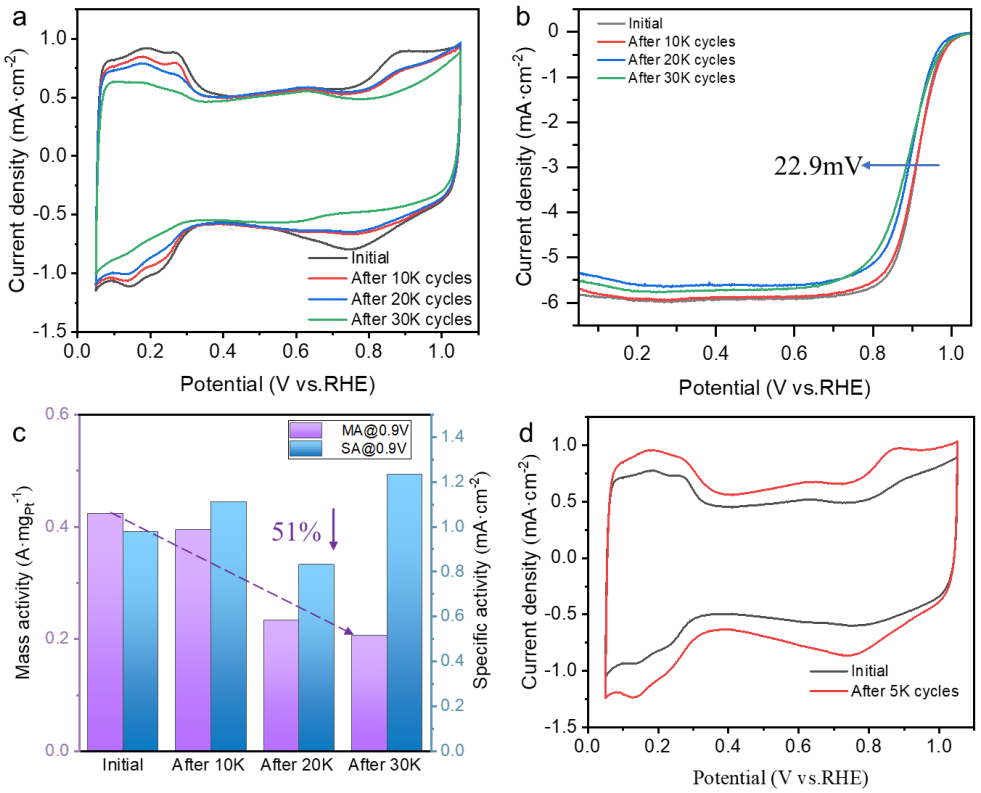

Fig. S6. (a) Cyclic voltammograms before and after different cycle tests in Ar-saturated electrolyte (50 $mV \cdot s^{-1}$), (b) Polarization curves before and after different cycle tests in O_2-saturated electrolyte (5 $mV \cdot s^{-1}$), (c) SA and MA before and after different cycle tests and (d) Cyclic voltammograms before and after 5000 cycles in a high potential range of 1.0–1.5 V for PtNi/KBC-600 in O_2-saturated electrolyte.

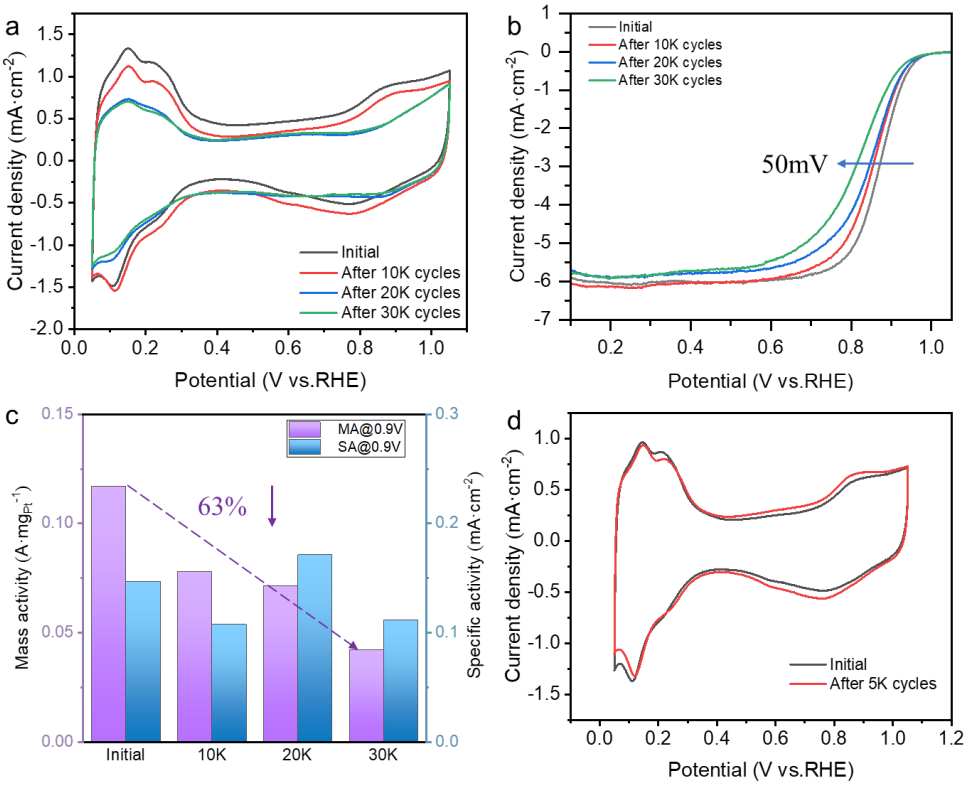

Fig. S7. (a) Cyclic voltammograms before and after different cycle tests in Ar-saturated electrolyte (50 $mV \cdot s^{-1}$), (b) Polarization curves before and after different cycle tests in O_2-saturated electrolyte (5 $mV \cdot s^{-1}$), (c) SA and MA before and after different cycle tests and (d) Cyclic voltammograms before and after 5000 cycles in a high potential range of 1.0–1.5 V for 20% Pt/C in O_2-saturated electrolyte.

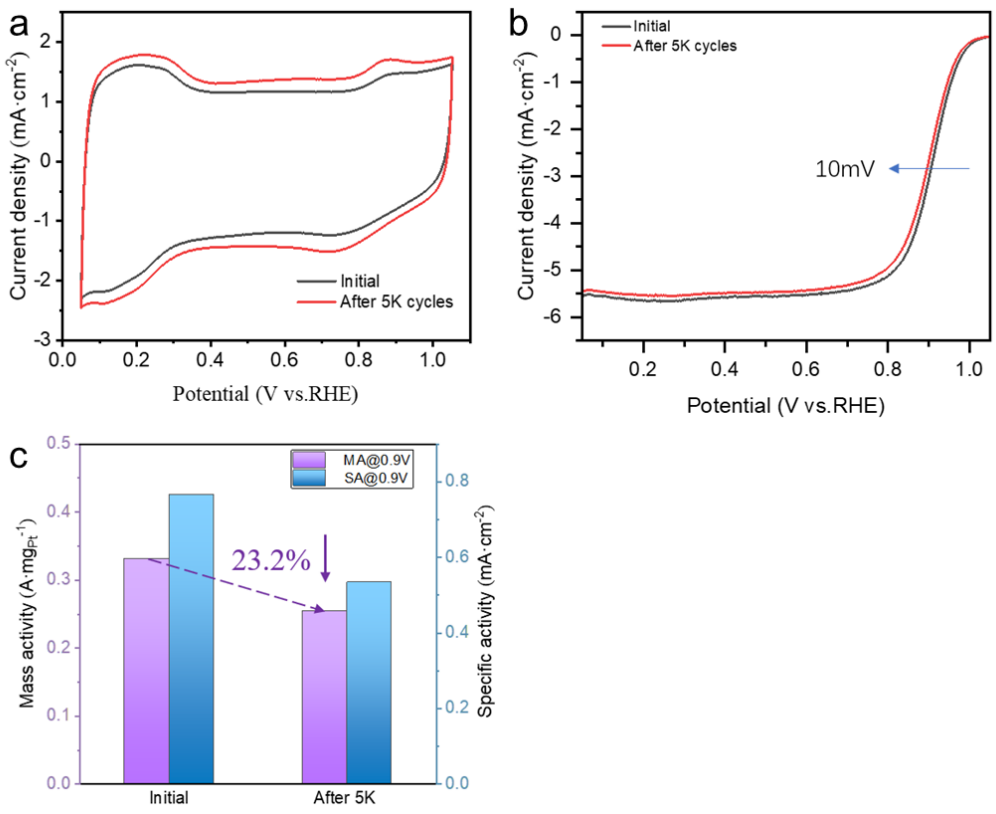

Fig. S8. (a) Cyclic voltammograms in Ar-saturated electrolyte (50 $mV \cdot s^{-1}$), (b) polarization curves in O_2-saturated electrolyte (5 $mV \cdot s^{-1}$) and (c) MA and SA before and after 5000 cycles in a high potential range of 1.0–1.5 V for PtNi/CNF-800.

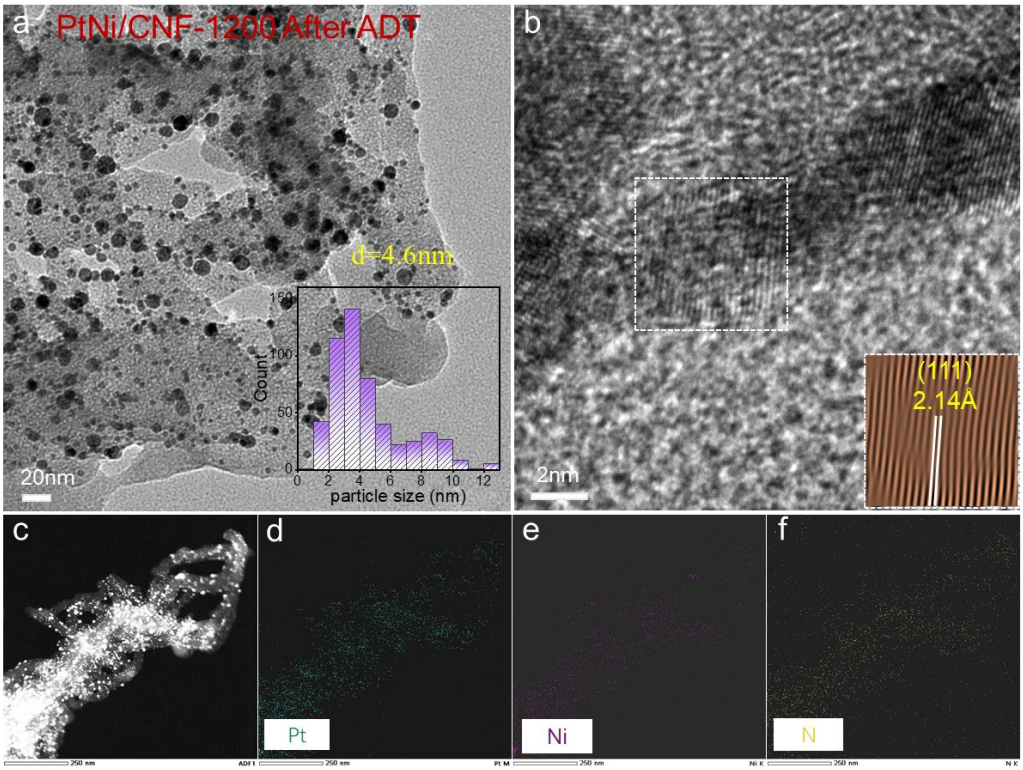

Fig. S9. (a) HRTEM image and particle size distribution (inset), (b) HRTEM image, the inset shows the corresponding information about lattice fringes, (c) HRTEM image and (d-f) energy-dispersive X-ray spectroscopy (EDS) mapping for PtNi/CNF-1200 after 5000 cycles in a high potential range of 1.0–1.5 V in O_2-saturated 0.1 M $HClO_4$ electrolyte.

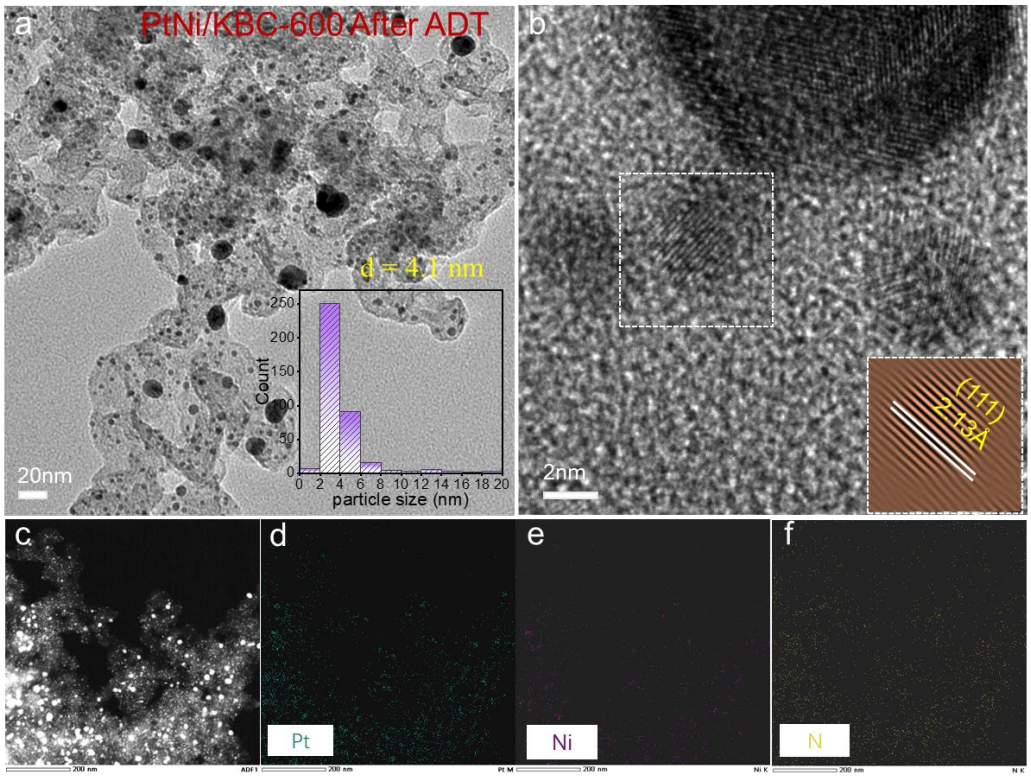

Fig. S10. (a) HRTEM image and particle size distribution (inset), (b) HRTEM image, the inset shows the corresponding information about lattice fringes, (c) HRTEM image and (d-f) energy-dispersive X-ray spectroscopy (EDS) mapping for PtNi/KBC-600 after 5000 cycles in a high potential range of 1.0–1.5 V in O_2-saturated 0.1 M $HClO_4$ electrolyte.

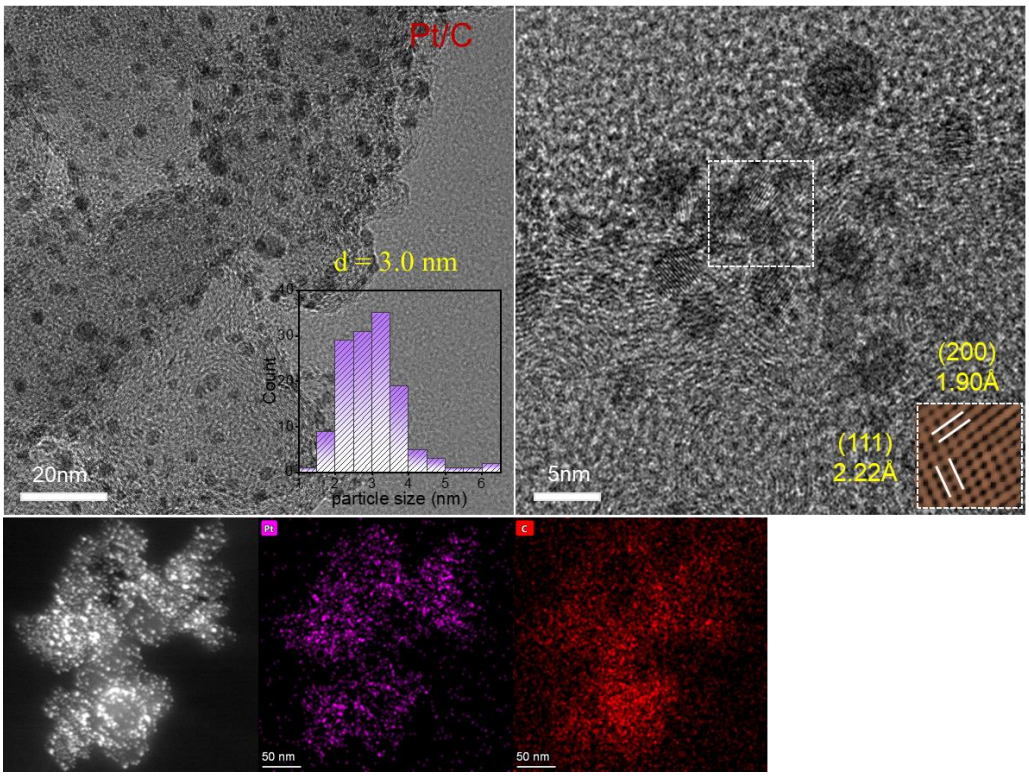

Fig. S11. (a) HRT EM image and particle size distribution (inset), (b) HRTEM image, the inset shows the corresponding information about lattice fringes, (c) HRTEM image and (d-e) energy-dispersive X-ray spectroscopy (EDS) mapping for 20% Pt/C.

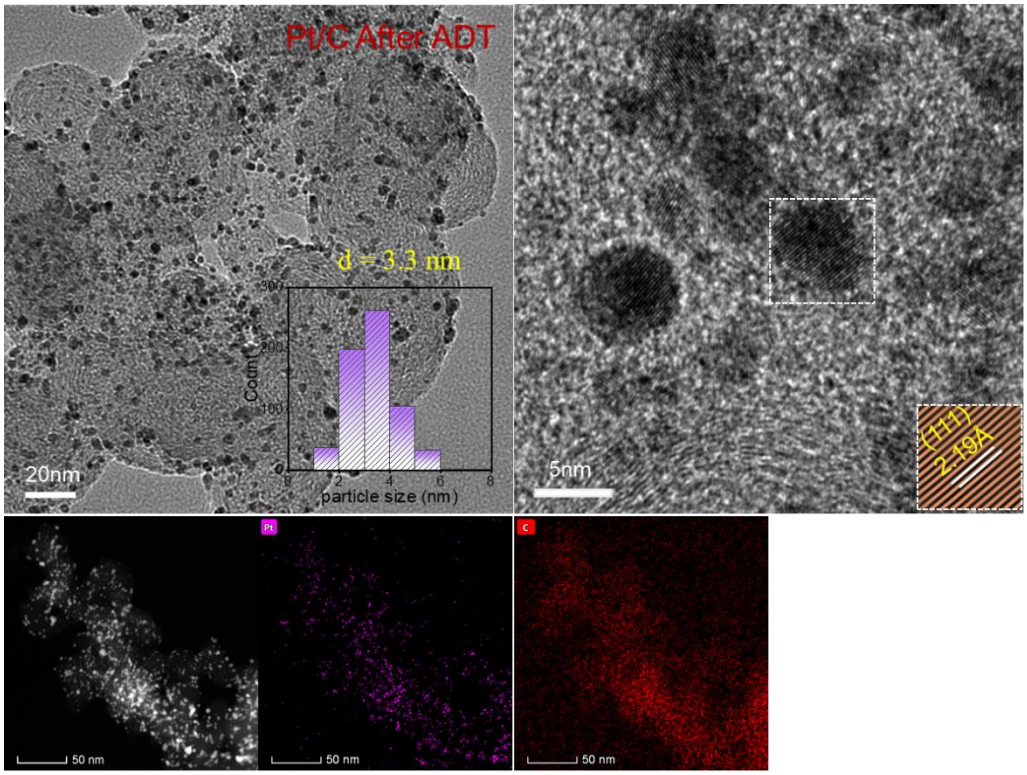

Fig. S12. (a) HRTEM image and particle size distribution (inset), (b) HRTEM image, the inset shows the corresponding information about lattice fringes, (c) HRTEM image and (d-e) energy-dispersive X-ray spectroscopy (EDS) mapping for 20% Pt/C after 5000 cycles in a high potential range of 1.0–1.5 V in O_2-saturated 0.1 M $HClO_4$ electrolyte.

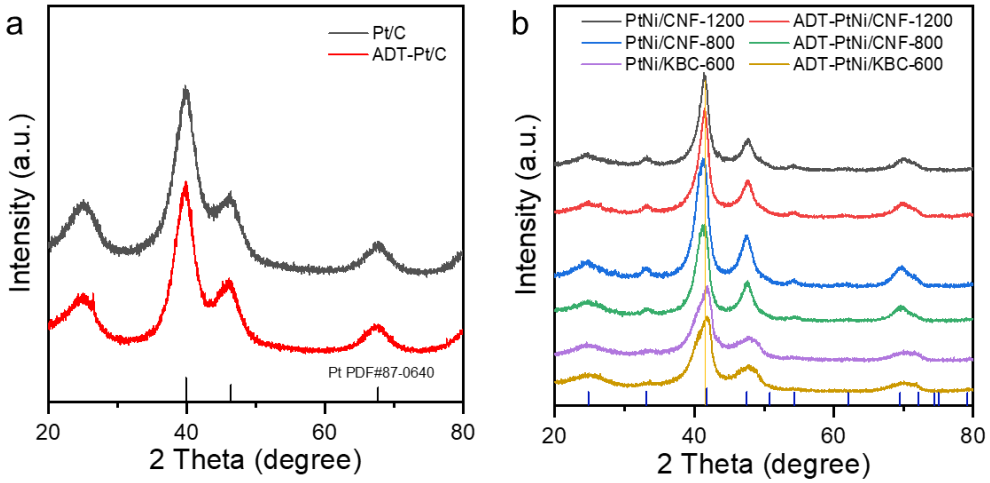

Fig. S13. (a) XRD patterns for 20% Pt/C before and after 5000 cycles in a high potential range of 1.0–1.5 V in O_2-saturated 0.1 M $HClO_4$ electrolyte. (b) XRD patterns for PtNi/CNF-1200, PtNi/CNF-800, and PtNi/KBC-600 before and after 5000 cycles in a high potential range of 1.0–1.5 V in O_2-saturated 0.1 M $HClO_4$ electrolyte.

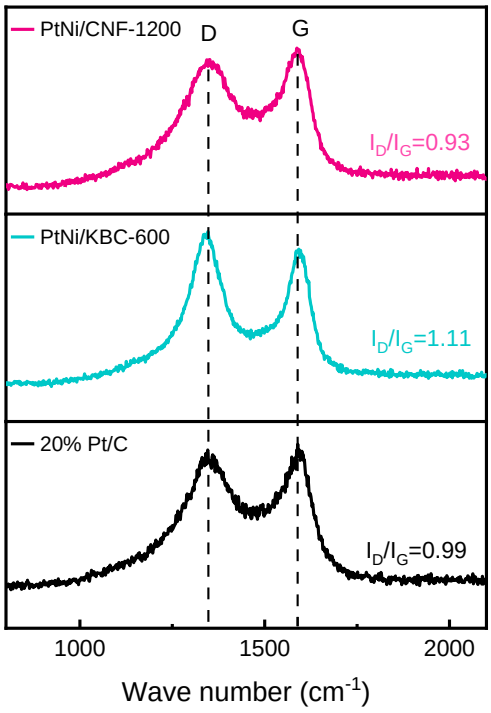

Fig. S14. Raman spectra for PtNi/CNF-1200, PtNi/KBC-600, and 20% Pt/C after 5000 cycles in a high potential range of 1.0–1.5 V in O_2-saturated 0.1 M $HClO_4$ electrolyte.

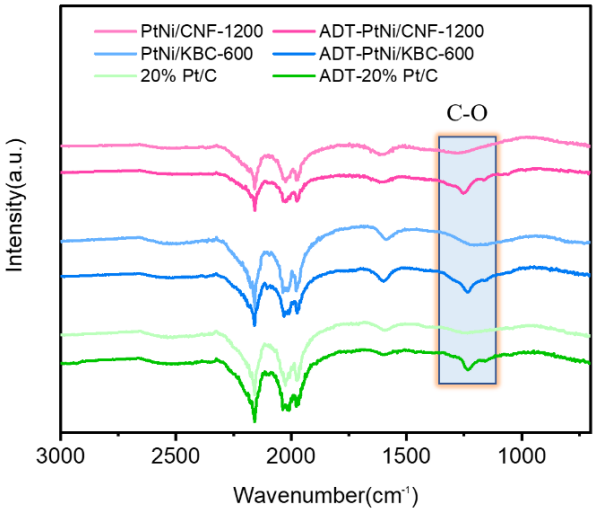

Fig. S15. FTIR spectrum for PtNi/CNF-1200, PtNi/KBC-600, and 20% Pt/C before and after 5000 cycles in a high potential range of 1.0–1.5 V in O_2-saturated 0.1 M $HClO_4$ electrolyte.

Table S1. Comparison of C, N and O contents in PtNi/CNF-1200 and PtNi/KBC-600 according to XPS data

Elements	C (wt%)	N (wt%)	O (wt%)
PtNi/CNF-1200	87.50	2.03	10.47
PtNi/KBC-600	91.69	0.86	7.45
20% Pt/C	95.03	-	4.97

Table S2. The atomic content of different types of carbon species derived from XPS data for PtNi/CNF-1200, PtNi/KBC-600, and Pt/C before and after the ADTs.

C 1s	Name	C–C	C–O	C=O	π-π*satellite
	Binding energy (eV)	284.80	285.50	289.50	291.50
PtNi/CNF-1200	at% (Before ADT)	50.30	37.52	12.18	-
	at% (After ADT)	45.91	26.38	9.30	18.41
PtNi/KBC-600	at% (Before ADT)	54.70	30.77	14.53	-
	at% (After ADT)	49.08	39.62	8.98	2.32
20% Pt/C	at% (Before ADT)	68.88	29.87	1.25	-
	at% (After ADT)	60.24	19.37	9.64	10.75

Table S3. EDS results of PtNi/CNF-1200 and PtNi/KBC-600.

Elements	Pt (wt%)	Ni (wt%)	N (wt%)
PtNi/CNF-1200	80.53	10.22	9.25
PtNi/KBC-600	86.89	11.47	1.64